S-Gear Design Rules

Jože Hlebanja, Gorazd Hlebanja, Mark Umberger

Abstract:
Gears featuring the curved path of contact were implemented in heavy industry where it was proven that such gears can successfully replace involute gears. Purely graphical method of design was later replaced by an analytical definition which enabled calculation of not only gear geometry but other relevant aspects as well (e.g. sliding velocity, curvature radii, etc). So, the most important definition is that of the rack profile which can be regarded as a cutting tool profile. Thus, the tooth flank of the rack profile defines the unique path of contact. And according to the law of gearing gears (external and internal) of arbitrary number of teeth are derived from there. Furthermore, the paper describes helical gears and crossed (perpendicular) helical gears which can be used in multiplicators.

Keywords:
power transmission, involute gears, S-gears, helical gears, crossed helical gear pairs

Introduction to the development of S-gears

Gears are machine elements of vital importance for the transmission of power from high-speed rotating power sources to work machines consuming the power. The shape of tooth flanks is decisive for seamless transmission of power from driving gears to driven gears. In modern gear manufacturing, a gear is generated using a basic-rack-shaped cutter whose datum line executes rolling motion on the gear's pitch circle. Shaping the tooth flanks requires a properly shaped generating cutting tool. Since Leonard Euler (1707–1783), the most common shape of cylindrical gear tooth flanks has been the involute, generated using a straight cutting edge and yielding a straight path of contact. *Fig. 1* shows the involute function: the curve begins in point K on the base circle and takes shape as point K unwinds from it. The centres of curvature in points 1, 2, 3 etc. on the involute are situated in corresponding points 1, 2, 3 etc. on the base circle. It is evident that the distances between the points on the base circle are increasing, and thereby also the involute's curvature radii. Following the involute in the other direction towards the base circle, the curvature radii are diminishing, finally reaching zero in point K. The contribution of the involute teeth flank's dedendum part in the transmission of power is therefore low. As a driving gear tooth meshes with a driven gear tooth, the transmission of power from the driving gear to the driven gear takes place on the A-E line, also called the path of contact. In involute gears, power (load) is transmitted from a small tooth flank surface in the dedendum part of the driving gear to a large tooth flank surface in the addendum part of the driven gear. This is unfavourable in terms of gear durability.

Prof. em. Dr. Jože Hlebanja, univ. dipl. inž., University of Ljubljana, Faculty of Mechanical Engineering, Slovenia
Dr. Gorazd Hlebanja, univ. dipl. inž., University of Novo mesto, Faculty of Mechanical Engineering, Slovenia
Dr. Mark Umberger, univ. dipl. inž., Entia, d. o. o., Ljubljana, Slovenia

S-gear design

The rules of S-gear design were presented for the first time in 2010 at the VDI International Conference on Gears in Garching near Munich in the paper "Spur gears with a curved path of contact for small gearing dimensions", published in "VDI Berichte 2108, VDI Verlag (p. 1281–1294)" [1]. These rules are often used in research work, so it may be assumed that they are well-known. In this paper, they will be reiterated and complemented with new findings. Both the previously mentioned work and this paper focus on the industrial gear manufacturing processes employing the rolling motion of cutters in the shape of the basic rack, where a point P_i on the generating tool's cutting edge moves towards point U_i on the path of contact. The location of point U_i obeys the basic law of gearing and here point G_i is generated (cut) on the emerging gear tooth flank. This is followed by rotating the gear tooth flank with the new point G_i in the direction of generation, so that point P_i travels from point U_i to the original point on the basic rack profile curve.

The described procedure for shaping S-gears is also assumed here, but our focus will be on larger gear dimensions and on the review of the state-of--the-art in S-gears. The starting points are our guidelines from the paper discussing smaller gears [1] and the equation for the rack tooth flank profile:

$$y_{Pi} = a_p \left(1 - (1 - x_{Pi})^n\right) \quad (1)$$

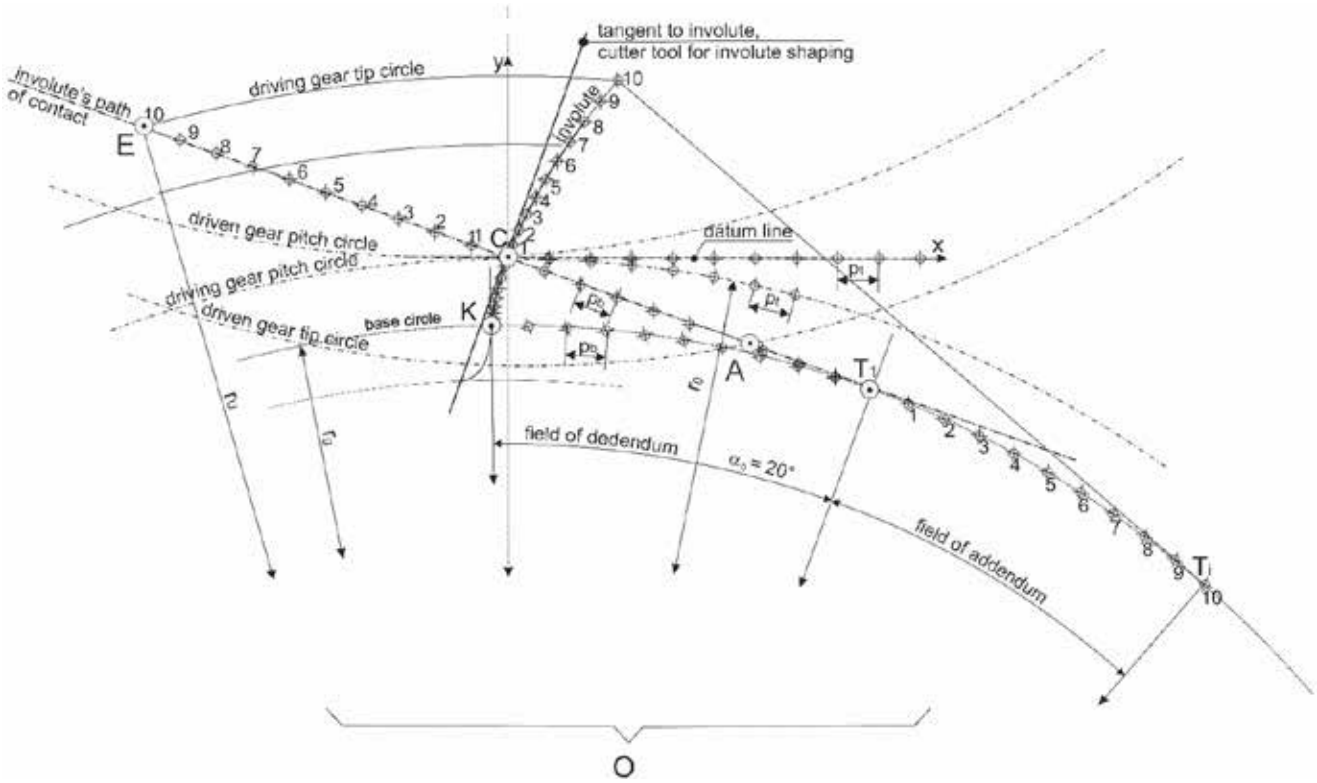

Figure 1 : *Kinematic conditions in the involute gear pitch point*

The function consists of two identical halves, one defining the addendum part of the rack tooth flank profile and the other its dedendum part. To every part of the cutting edge there belongs a corresponding section of the path of contact. The whole path of contact assumes the shape of the letter "S", and this gear type was therefore named "S-gears"/"S--gearing".

The cutting edge function (1) assumes the maximum value $y_V = a_p$ at $x_V = m$ and the part of function used to define the basic rack tooth flank is from C to A(x_{Pa}, $y_{Pa} = m$). The abscissa x_{Pi} of any point P_i on the basic rack profile is determined by:

$$x_{Pi} = 1 - (1 - y_{Pi}/a_p)^{1/n} \qquad (2)$$

The derivative y'_{Pi} is used to obtain the tangents on the cutting edge curve:

$$y'_{Pi} = n \cdot a_p \cdot (1 - x_{Pi})^{n-1} \qquad (3)$$

Here, x_{Pi} and y_{Pi} are the Cartesian coordinates with the origin in the pitch point C, a_p is the size factor

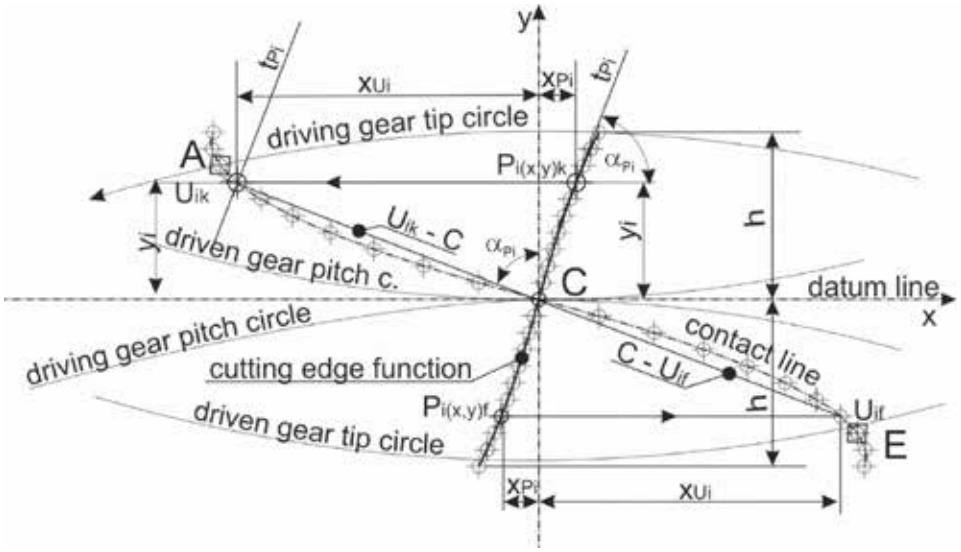

Figure 2 : *Cutting edge function and the corresponding path of contact*

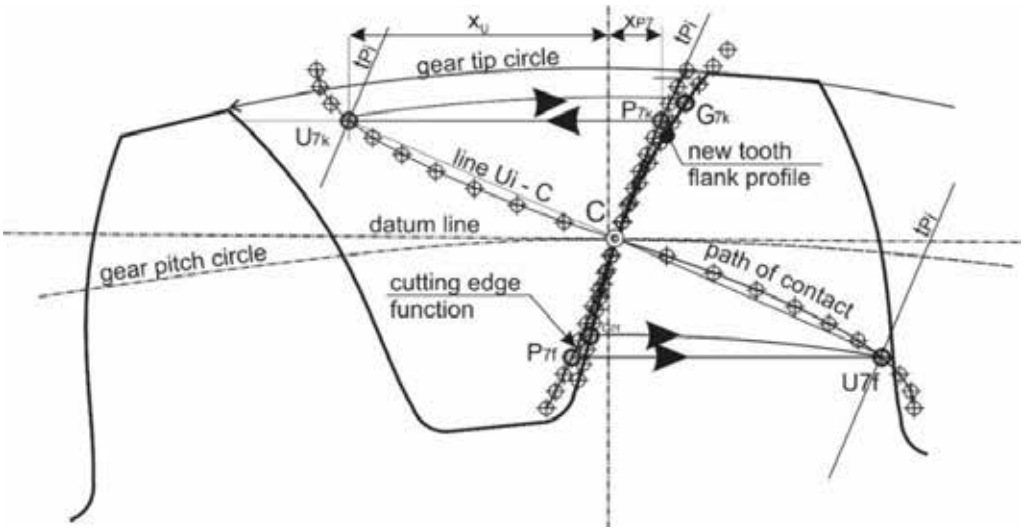

Figure 3 : *Generation of points Gi on the tooth flank takes place at the location of points Ui on the path of contact*

and n is the exponent. Both parameters are decisive for the characteristics of the profile function y_{Pi}. Two halves join in the pitch point C to form a single function y_{Pi}. The coordinates of points in the dedendum part are of identical magnitude, but their sign is reversed. In any point P_i on the profile, a tangent t_{Pi} can be drawn with slope $\alpha_{Pi} = \text{atan}(y'_{Pi})$. As the rack cutter moves horizontally, it reaches the point U_i on the path of contact, in which the normal to tangent t_{Pi} crosses the pitch point C. The tooth flank thereby satisfies the fundamental law of gearing. The abscissa x_{Ui} of point U_i on the path of contact is determined from the ordinate y_{Pi} and the slope of the tangent α_{Pi}:

$$x_{Ui} = y_{Pi} \cdot \tan(\alpha_{pi}) = -y_{Pi} \cdot y'_{Pi} \quad (4)$$

The process of machining the workpiece in points U_i with the cutting edge generates the tooth flank surface along the path of contact as determined by Eq. (1).

To calculate the velocity of every point G on the tooth flank while on the path of contact U_i, the radius r_{Ui}, i.e. the distance from the gear centre, is needed:

$$r_{Ui} = (x_{Ui}^2 + (r_0 \pm y_{Ui})^2)^{0,5}, \quad (5)$$

where r_0 is the radius of the gear pitch circle. Eq. (5) is valid for the addendum part (plus operator in the parentheses) and the dedendum part (minus operator in the parentheses) of both the driving and the driven gear.

Shaping S-gear tooth flanks

As the point P_i on the cutting edge reaches the path of contact in point U_i (Fig. 2, 3, and 4), profile generating takes place on the workpiece and point G_i emerges on the gear tooth flank. The point G_i on the gear must travel the path s until it reaches the cutting point U_i:

$$s = x_{Pi} + x_{Ui} \quad \text{(Fig. 2)} \quad (6)$$

The new point on the tooth flank Gi also travels the same path over a circular arc until it reaches the final position on the gear. The arc angle φ_{0UGi} is determined as follows:

$$\varphi_{0UGi} = s/r_0 = (x_{Pi} + x_{Ui})/r_0 \quad (7)$$

Generating S-gear tooth flanks by milling

The starting points for generating S-gear tooth flanks by milling are a composition of the cutting edge and the path of contact as shown and functionally linked in Fig. 2, 3 and 4, the requirement for the cutting edge profile function to satisfy Eq. 1, and tooth flank generation by rolling motion. In this case, the points P_i on the cutting edge generate points G_i on the tooth flank of the gear being cut, the machining itself taking place in points U_i on the path of contact. The location of points G on the finished teeth flanks is determined by coordinates x_{Gi} and y_{Gi} for the tooth addendum part:

$$x_{Gi} = r_{Ui} \cdot \sin \varphi_{Gi}, \; y_{Gi} = r_{Ui} \cdot \cos \varphi_{Gi} - r_0 \quad (8)$$

The coordinates x_{Gj} and y_{Gj} for the dedendum part are pole-symmetric.

The derivation of equation (8) is explained using *Fig. 4* showing the most important design features.

Gear tooth flank profile calculation procedure

First, the cutting edge's basic function as defined in [1] is calculated using real data:

1. The size factor a_p is selected from the range

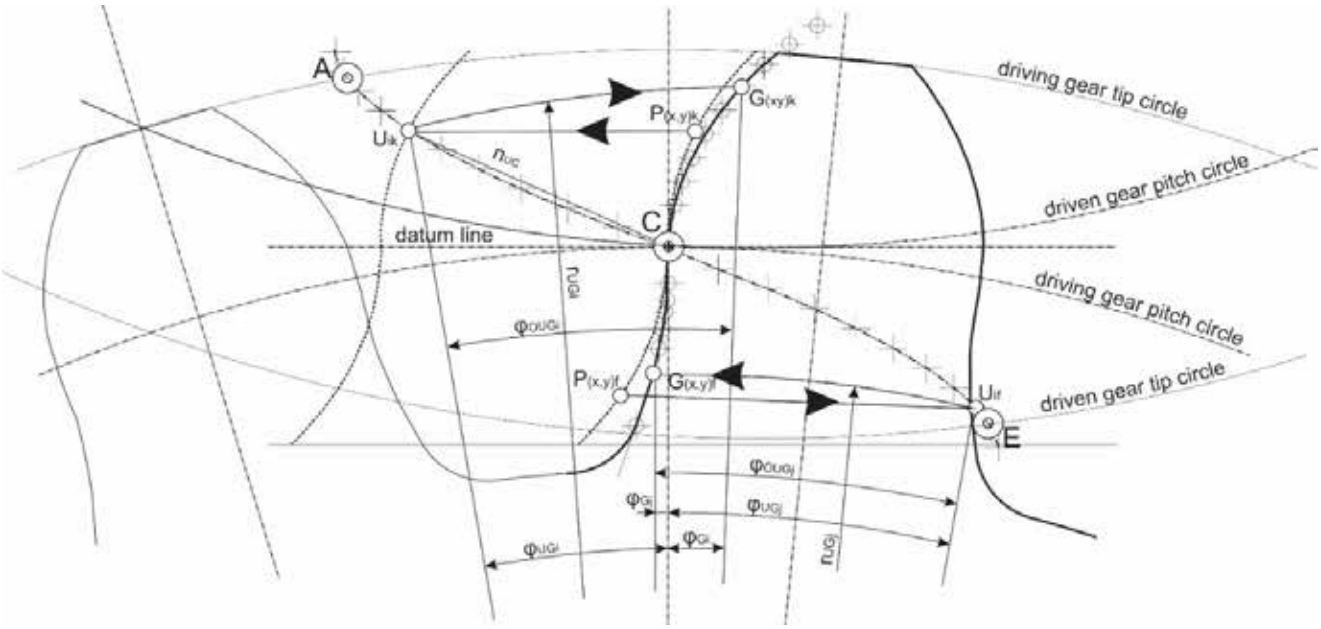

Figure 4 : *Geometric parameters defining the gear tooth flanks*

1,2–1,6; recommended value is a_p = 1,4.

2. Value for α_0 is selected: α_0 = 70°, tan(α_0) = 2,747
3. The radius of gear pitch circle r_0 is determined; r_0 = z·m/2 (z = number of teeth, m = module)
4. The ordinates y_i of points P_i are determined along the addendum part of the cutting edge: 10 points P_i were distributed between the tooth tip and point C in 0,1 mm intervals. The profile is invariant to the module, e.g. for m = 5 mm these intervals are multiplied by 5.
5. In the dedendum part of the tooth, the point ordinates y_i are distributed using the same intervals, but in the reverse direction from point C to the bottom of the fillet.
6. The abscissa x_i is calculated for all points P_i using Eq. 2.
7. The derivative y_i' is calculated for all points P_i using Eq. 3.
8. The abscissas x_{Ui} of all points on the path of contact U_i are calculated using Eq. 4.
9. The radii r_{Ui} (distance from the gear centre) in respective points U_i on the path of contact are calculated using Eq. 5.
10. The angles φ_{OUGi} and φ_{OUGj} are calculated for the addendum and dedendum part of the tooth, respectively.
11. The angles φ_{UGi} and φ_{UGj} are calculated for the addendum and dedendum part, respectively.
12. The angles φ_{Gi} and φ_{Gj} are calculated for the addendum and dedendum part, respectively.

Using the data obtained under points 1 to 12 and Eq. 8, the coordinates of the points on the gear tooth flank $G_i(x, y)$ are calculated for all points P_i on the cutting edge (10 points for the addendum and 10 points for the dedendum part):

(9a)

$$\varphi_{0UGi} = (x_{Pi} + x_{Ui})/r_0;\ \varphi_{UGi} = \text{atan}(x_{Ui}/(r_0 + y_i));\ \varphi_{Gi} = \varphi_{0UGi} - \varphi_{UGi}$$

In the root part, the flank is generated before the tooth bisector and the following angles are formed:

(9b)

$$\varphi_{0UGj} = (x_{Uj} - x_{Pj})/r_0;\ \varphi_{UGi} = \text{atan}(x_{Uj}/(r_0 - y_j));\ \varphi_{Gj} = \varphi_{0UGj} - \varphi_{UGj}$$

Slope of tangent α_{kGt} in points $G_i(x, y)$ on the new tooth flank profile

Considering the selected base tooth profile, the value of tangent slope in any point P_i on the curve can be determined as y'_{Pi}, yielding the slope of the tangent α_{kGt} in any point G_i on the tooth flank as follows for the addendum part:

$$\alpha_{Gi} = \text{atan}(y'_{Pi}) - \varphi_{0UGi} \qquad (10a)$$

and for the dedendum part:

$$\alpha_{Gi} = \text{atan}(y'_{Pj}) + \varphi_{0UGj} \qquad (10b)$$

The slope of the tangent Υ on the cutting edge in pitch point C is particularly important and values between 65° and 75° are usually used. The slope of the tangent in the pitch point (x_{Pi} = 0) is as follows:

$$\tan \Upsilon = n \cdot a_p \cdot (1 - x_{Pi})^{1/n} = n \cdot a_p$$

The exponent n corresponding to the selected value of a_p = 1,4–1,5 is therefore:

$$n = \tan \Upsilon / a_p \qquad (11)$$

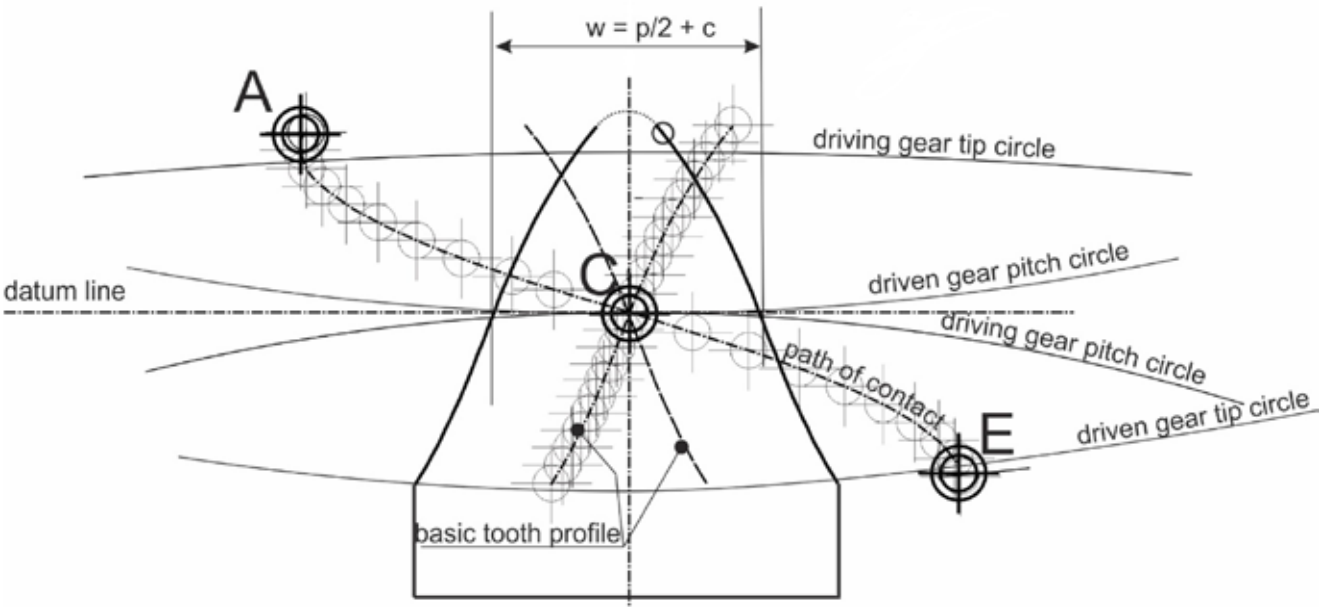

Figure 5 : *Profile of the cutter used for machining S-gear tooth spaces*

The shape of cutters for the S-gear tooth spaces

The profile of cutters as shown in *Fig. 5* is determined from the cutting edge function and the path of contact, Fig. 3, passing through the pitch point C. The right-hand cutting edge on Fig. 5 was used to generate the left-hand flank of the tool, while its mirrored counterpart, which also passes through the pitch point C, was used to obtain the right-hand flank of the cutting tool. The distance between both tooth flanks equals the tooth space w, consisting of half the pitch p plus the gear's operating backlash c, as determined by the standard.

Fig 6. shows an S-gear pair designed according to the procedure presented in this paper. The driving gear has 16 and the driven pinion 40 teeth. The path of contact intersects the driving gear's tip circle in point A. Here the root of the driving gear tooth starts engaging with the tip of the driven gear. The path of contact ends in point E where it intersects

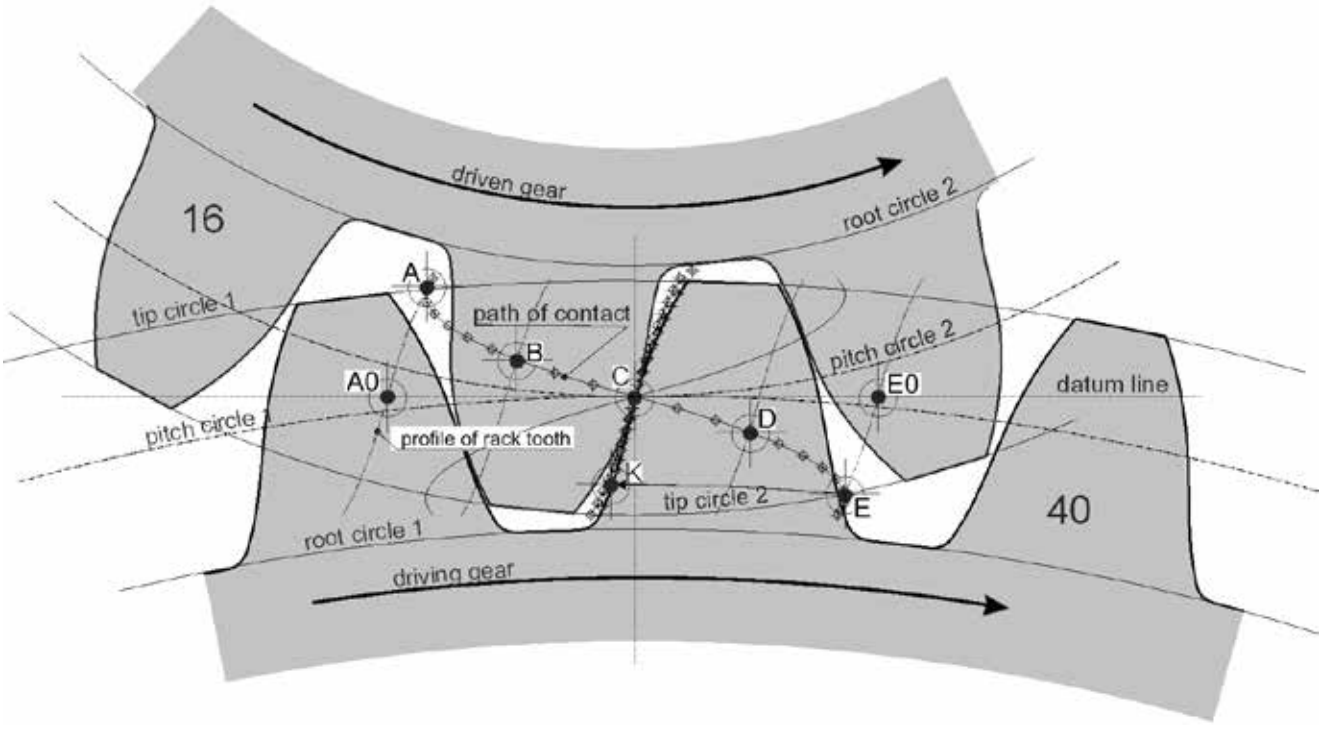

Figure 6 : *S-gear pair teeth, m = 5 mm (enlarged)*

the driven gear's tip circle. The length of the path of contact depends on the gear module. In this pair, both gears have the same module and they therefore share a path of contact of the same shape and length. Power is transmitted by rolling motion of the driven gear's flank on the driving gear's flank. In contrast, in involute gears the point of contact in the pitch point C is stationary and the tooth flanks are sliding in the direction of the helix.

Helical S-gears

Ordinary helical gears are characterised by an involute tooth flank profile in the plane perpendicular to the axis. Their teeth are set at an angle relative to the axis and take the shape of a helix with helical spaces in between. This section presents the new helical S-gears.

The left-hand side of *Figure 7* shows a section through the teeth and the spaces of a helical S-gear through the pitch point C plane and the datum line, the direction of generation by rolling motion and the direction of tooth space milling executed by the rack teeth. The right-hand side of Figure 7 right shows a vertical section A-E through the helical gear and the tooth space profile in the direction of reciprocating generating motion. It also shows the path of contact in the same plane, beginning in point A and ending in point E. The path of contact begins at the tip circle of the driving gear (A) and ends at the tip circle of the driven gear (E). The abscissas of points U_i on the path of contact are multiplied by 1/cos β when using this method. It must be noted that milling generates points G on the new gear flanks along the whole path of contact, removing material over the length of the flank.

Friction testing of S-modified gear pairs with identical paths of contact

The main advantage of S-modified gear pairs lies in the fact that the relative motion in contact points on the tooth flanks is rolling and friction is largely absent, all the way from the start of meshing in point A to the end of engagement in point E.

The helical S-gears presented in this paper were milled using a corresponding custom-made cutter whose datum line executed rolling motion on the gear's pitch circle. The profile of the custom-made cutters used to machine the tooth spaces was constructed following the S-gear design rules, Fig. 2, 3 and 4. Company Perovšek, d.o.o. manufactured the gears on ordinary gear-milling machines. Both gears in a pair were manufactured using the same tool to obtain the same path of contact.

The test bed consisted of the driving gear fitted on the output shaft and the driven gear fitted on the

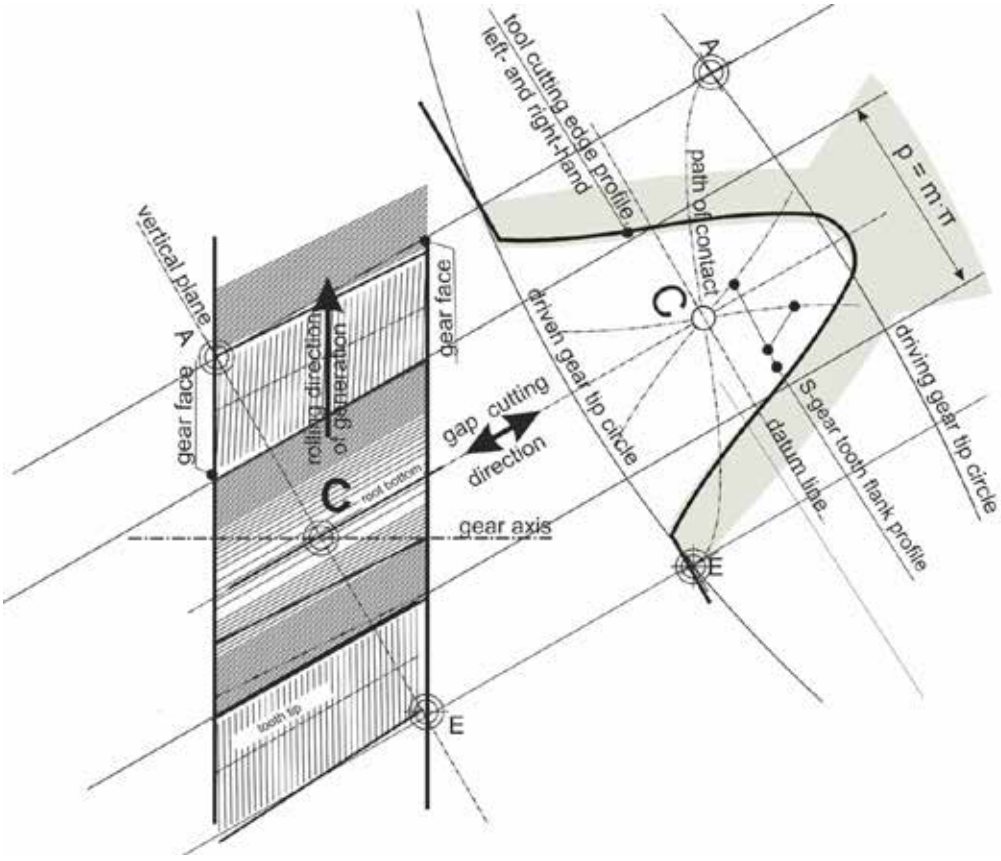

Figure 7 : *Characteristics of helical S-gear manufacturing*

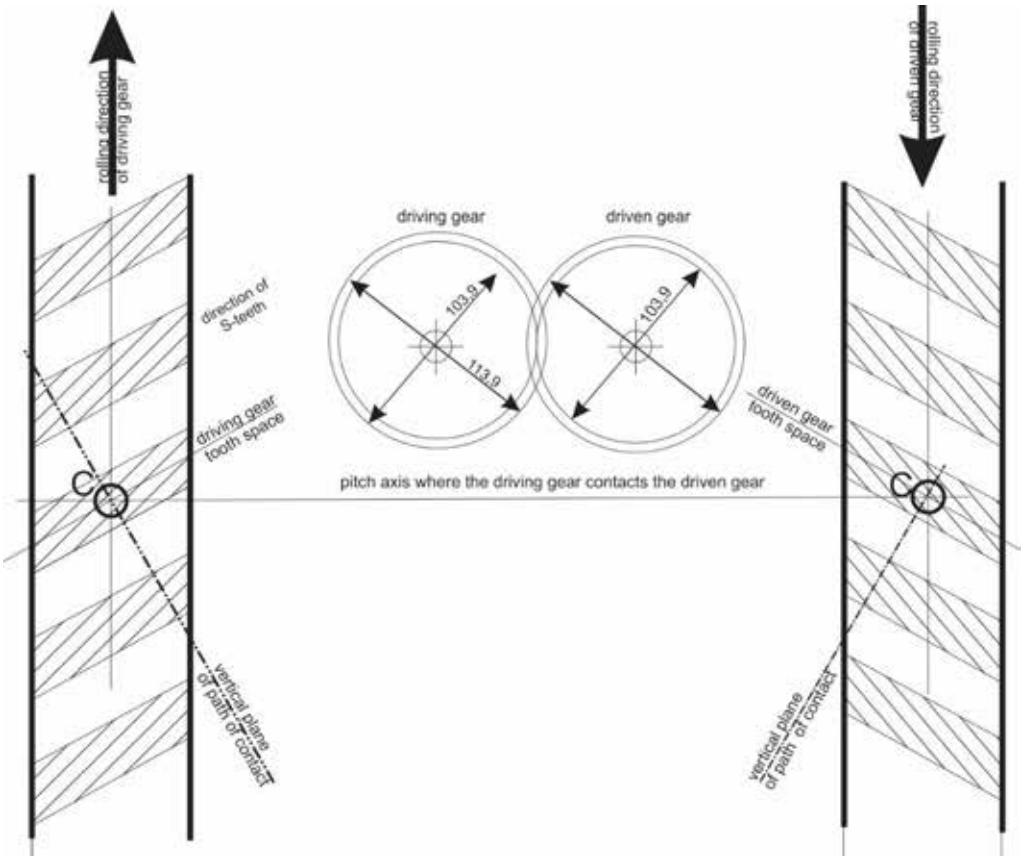

Figure 8 : *Test of resistance to rotation of modified S-gears under no external load*

Figure 9 : *A different test helical S-gear pair: driving gear $z_1 = 28$, driven gear $z_2 = 16$*

Figure 10 : *A helical S-gear pair with perpendicular shafts as used in centrifuges*

input shaft. Friction losses in the gear transmission were monitored and they turned out to be negligible. It was therefore confirmed that this gear pair transmits torque by rolling motion on the path of contact, thereby saving energy. *Fig. 8* shows corresponding shematics and *Fig. 9* a prototype helical gear pair.

Helical gear pairs with perpendicular shafts

This gear drive type consists of two cylindrical gears with helical teeth fitted to perpendicular shafts. They are often used in centrifuge drives (e. g. Alfa-Laval) and our implementation uses a large driving gear with 60 teeth on the horizontal shaft and a smaller driven gear with 20 teeth on the vertical shaft, *Fig. 10*. The module of our gear mechanism is m = 5 mm, the angle of left-hand helix angle on the large driving gear is $b_1 = 30°$, and the right-hand helix angle on the small driven gear is $b_2 = 60°$. Our goal was to test the manufacturability of such S-gears and the resulting gear pair shown in Fig. 10 proved to be a success.

Conclusions

In this paper we have presented the design and the essential elements of our S-gears that were under development for more than 10 years and are now feasible for industrial manufacturing. Previous research of S-gears focused mainly on smaller steel or plastic gears with modules m ≤ 1 mm, while present work also covers larger gears. The presented subject matter does not claim to be complete, but the author believes that the gear specialists may find it useful and will be able to complement it as necessary. The author is also ready to answer any questions. He believes that S-gears will be able to fill some niches where involute gears are not a good fit and wishes a lot of success to all users of S-gears.

References

[1] Hlebanja, J., Hlebanja, G. (2010). Spur gears with a curved path of contact for small gearing dimensions. VDI-Bericht 2108: 4th International Conference on Gears, Garching near Munich, Germany, Oct. 4-6, 2010: Europe invites the world. VDI-Verlag, Düsseldorf, p. 1281–1294.

[2] Hlebanja, J. (1974). Erzeugung von Zahnflank-

Nomenclature

Figure 1	
AE	path of contact
C	pitch point
K	involute function start point
T_1	center of involute curvature radius in point C
T_i	center of involute curvature radius in point i
r_U	tip circle radius
r_g	base circle radius
Figure 2	
P_i	point on the rack profile (cutting edge)
U_i	point on the path of contact
$U_{ik}C$ and CU_{jk}	normal to tangent t_{Pi}
t_{Pi}	tangent to cutting edge in point P_i
α	angle of tangent t_{Pi}
h	tooth tip/root height
Figure 3	
U_{7k}, U_{7f}	points on path of contact where points G_{7k} and G_{7f} are generated
Figure 4	
$\varphi_{OUGi,\,j}$	angle of circular arc between $U_{ik,f}$ and $G_{k,\,f}$
$\varphi_{UGi,\,j}$	angle of circular arc between $U_{ik,f}$ and axis y
$\varphi_{Gi,\,j}$	angle of circular arc between $G_{k,f}$ and axis y
$r_{UGi,\,j}$	radius in point $G_{i,\,j}$
Figure 5	
p	pitch
c	backlash
w	tooth space
Figure 6	
x_i, y_i	Cartesian coordinates originating in the pitch point C
a_p	size factor
n	exponent
α_{Pi}	slope of tangent t_{Pi}
r_{Ui}	radius in point U_i, measured from the gear centre
r_0	pitch circle radius
φ_{OUGi}	arc of travel of point G_i
φ_{Gi}	slope of tangent t_{Gi}

enprofilen durch Rollkurven. Antriebstechnik, vol. 13, no. 2, p. 111-117.
[3] Hlebanja, J. (1991). Influence of the path of contact shape on sliding conditions between tooth flanks. JSME International conference on motion and power transmission, Hiroshima
[4] Hlebanja, J. (1976). Konkav-konvexe Verzahnung. Ermittlung der Zahnflanken und einige Grenzfälle. Antriebstechnik, vol. 15, no. 6, p. 324–329.
[5] Niemann G., Winter H. (1988). Maschinenelemente, Band 2, chapter Sonderverzahnung nach Hlebanja, p. 43.
[6] Hlebanja J, Okorn I. (1996). Investigation of tooth surface durability of non-involute spur gears. Proceedings of International Conference on Gears, p. 443–450.
[7] Hlebanja J, Okorn I. (1999). Charakteristische Eigenschaften von Zahnrädern mit stetig gekrümmter Eingriffslinie. Antriebstechnik, vol. 38, nr. 12, p. 55–58.
[8] Okorn I. (2000). Research of tooth flank durability of gears with progressively curved path of contact. Ph.D. Thesis (in Slovene). University of Ljubljana
[9] Hlebanja J., Hlebanja G. (2002). Lubrication efficiency of S-Gears. VDI-Bericht 1665. VDI-Verlag, Düsseldorf, p. 1065-1076.
[10] Hlebanja J., Hlebanja G. (2005). Tooth flank durability of internal S-gears. VDI-Bericht 1904. VDI-Verlag, Düsseldorf, p. 385–394.
[11] Hlebanja J., Hlebanja G. (2005). Anwendbarkeit der S-Verzahnung in Getriebebau. Antriebstechnik, vol. 44, nr. 2, p. 34–38.
[12] Hlebanja J., Hlebanja G. (2008). Constructive measures to increase the load-carrying capacity of gears, Proceedings of 48. anniversary of the Faculty of technical sciences, Novi Sad, Serbia.
[13] Hlebanja J., Hlebanja G. (2009). Konkav-konvexe Sonderverzahnung, Vorteile und Nachteile gegenüber Evolventenverzahnung. Proceedings of International Conference on Power Transmission '09
[14] Hlebanja G. (2011). Specially Shaped Spur Gears: A Step Towards Use in Miniature Mechatronic Applications. Proceedings of 7th International Scientific Conference on Research and Development of Mechanical Elements and Systems IRMES, p. 475-480
[15] Hlebanja G., Kulovec S., Duhovnik J. (2014). S-gears made of polymers. Proceedings of the 1st international conference on polymer tribology, Bled, Slovenia
[16] Zorko D., Kulovec S., Tavčar J., Duhovnik J. (2017). Different teeth profile shapes of polymer gears and comparison of their performance. Journal of Advanced Mechanical Design, Systems, and Manufacturing, vol 11, no. 6.
[17] Hlebanja G., Kulovec S. (2018). Thermal behaviour of plastic S-shaped gears in comparison with involute gears. Proceedings of 3rd international conference on polymer tribology, Portorož, Slovenia. This research was co-founded by the Republic of Slovenia and the European Regional Development Fund.
[18] Hlebanja G., Hlebanja J. (2013). Influence of axis distance variation on rotation transmission in S-Gears: example of heavy-duty gears, VDI-Bericht 2199, VDI-Verlag, Düsseldorf, p. 669-679.
[19] Hlebanja G., Kulovec S., Duhovnik J. (2016). Experimental determination of plastic S-gear characteristics. Proceedings of 2nd international conference on polymer tribology, Ljubljana, Slovenia.
[20] Duhovnik J., Zorko D., Sedej L. (2016). The effect of teeth profile shape on polymer gear pair properties. Tehnički vjesnik, vol. 23, no. 1., p. 199–207.
[21] Hlebanja G., Hlebanja J. (2012). Contact circumstances of the highly loaded , low speed gears, Proceedings of KOD 2012, p. 21–26.
[22] Hlebanja J., Hlebanja G. (1994). Efficiency and maximal transmitted load for internal lantern planetary gears. Proceedings of International gearing conference, p. 117-120.
[23] Hlebanja J., Hlebanja G. (1994). Planetary gearing. patent no. 9300152 with Slovenian Intellectual Property Office (SIPO).
[24] Hlebanja J., Hlebanja G. (2012). Contribution to the development of cylindrical gears. Proceedings of 4th international conference Power transmissions, Sinaia, Romania, p. 309–320
[25] Hlebanja G., Kulovec S., Hlebanja J., Duhovnik J. (2014). S-gears made of polymers. Ventil, vol 20. no. 5, p. 358–367

Dedication to Professor Winter (6. 1. 1921 – 14. 11. 1999)

Alternatives for involute gears have been sought in the expert circles for many years. Our idea to shape the cutting edge using a particular mathematical function proved to be successful to a certain extent. In my endeavours, I have enjoyed a lot of support from Prof. Prof. em. Dr.-Ing. Dr.-Ing. E.h. Hans Winter and his associates at FZG. Professor Winter was a world-renowned scientist in the field of development of gear technology and modern technical systems. Upon the presentation of this review of the state-of-the-art in S-gear development, the late professor Winter deserves all acknowledgement and the author expresses his appreciation for professor Winter's contribution to the development of gear technology.

Pravila za oblikovanje S-Ozobij

Razširjeni povzetek:
Zobniki z ukrivljeno ubirnico so bili izdelani za potrebe težke industrije pred več desetletji. Izkazalo se je, da lahko taki zobniki uspešno nadomestijo evolventne zobnike. Takratne grafične metode konstruiranja zobnikov in orodij pa je bilo nujno nadomestiti z analitičnimi metodami. Profil boka zoba zobnice predstavlja definicijo rezalnega orodja. Tako je bilo utemeljeno, da se bok zobnice definira s polsimetrično parabolično funkcijo. Funkcija vsebuje dva parametra, s katerima se lahko oblika te funkcije (posledično pa tudi oblika zob zobnika) spreminja. To sta eksponent in faktor velikosti. Za nek bok zoba zobnice obstaja zgolj ena sama ubirnica, iz nje pa lahko izpeljemo zunanje ali notranje zobnike s poljubnim številom zob. Iz praktičnih razlogov lahko modul jemljemo kot mersko enoto.

Posebej je poudarjena razlika med evolventnimi in S-zobniki, izkaže se namreč, da imajo med ubiranjem zob gonilnega pastorka z gnanim zobnikom evolventni zobniki razmeroma kratek korenski del pastorka z majhnimi krivinskimi radiji nasproti precej daljšim vrhom gnanega zobnika, kar je s stališča trajnosti takega zobnika neugodno.

V članku je natančno opisan postopek, kako pridemo od analitično definirane polsimetrične oblike boka zoba zobnice do ubirnice in zob dveh zobnikov s poljubnima številoma zob, ki ubirata. Pri tem je pomen definicije boka zoba zobnice v tem, da omogoča numerični izračun. To ne velja samo za obliko bokov zob in protizob, ampak tudi za računanje krivinskih radijev, drsnih hitrosti, bočnih tlakov, ocene minimalnega oljnega sloja, ocene t. i. bliskovne temperature, dela trenja itd., kar sicer v prispevku ni prikazano.

Poseben pomen ima oblika osnovnega orodja za zobčanje S-zobnikov, to je zobate letve. Pomembna je možnost uporabe istega orodja za zobnike s poljubnim številom zob in še posebej pri poševnih in poševnozobih zobnikih z mimobežnimi (v tem primeru pravokotno postavljenimi) osmi, t. i. vijačnimi zobniškimi pari.

Največja prednost S-ozobja je v tem, da je pri relativnem gibanju v kontaktu več kotaljenja in manj drsenja in posledično manj trenja. To velja tudi za poševnozobe zobnike. Izdelan je bil tudi prototip para jeklenih vijačnih zobnikov za multiplikator z mimobežnima pravokotnima osema z modulom 5 mm. Gonilni zobnik ima 60 zob in ß = 30°, gnani zobnik pa 20 zob in kot ß = 60°.

Ključne besede:
prenos moči, evolventni zobniki, S-zobniki, poševnozobi zobniki, vijačni zobniški par